JACS Au
AN OPEN ACCESS JOURNAL OF THE AMERICAN CHEMICAL SOCIETY

pubs.acs.org/jacsau
Article

Anomalously High Dielectric Strength and Capacitive Energy Density of Thin Entangled Glassy Polymer Films

Published as part of JACS Au special issue "Polymers for the Clean Energy Transition".

Maninderjeet Singh,* Saurabh Kr. Tiwary, Roushanak Nejat, Jack F. Douglas,* and Alamgir Karim*

Cite This: JACS Au 2025, 5, 121−135
Read Online

ABSTRACT: The influence of high-intensity electric fields on the stability of polymeric materials is a problem of interest in the design of next-generation energy storage and electronic devices, and for understanding the limits of stability of polymer films exposed to large electric fields generally. Here, we show that the dielectric strength of entangled glassy polymer films increases as an inverse power-law of the film thickness h for "ultrathin" films below a micron in thickness. The dielectric strength enhancement in these polymer films becomes as large as ≈2 GV/m in films thinner than 100 nm, but in this thickness regime, the increase of the dielectric strength depends strongly on the polymer mass, sample aging time, and the method of film preparation. The enhancement of the dielectric breakdown strength is attributed to the mechanical instability of the elastic film subjected to sufficiently large electric fields and a large, but not generally well-understood, enhancement of effective stiffness of entangled glassy polymer films subject to large deformations, an effect that has previously been observed to become greatly enhanced when such films are made thinner. As a proof of principle regarding applications, we utilize ultrathin glassy polymer films of the type studied in our paper to fabricate polymeric nanocapacitors having ultrahigh discharge energy densities (U_d^{max}) as large as 27 J/cm^3 and having efficiencies greater than 80%. These efficiency values at comparable charge densities are significantly higher than those of competing ferroelectric polymer materials, and we anticipate that our observations will inspire the creation of practical high-energy density nanocapacitor devices for advanced energy storage applications.

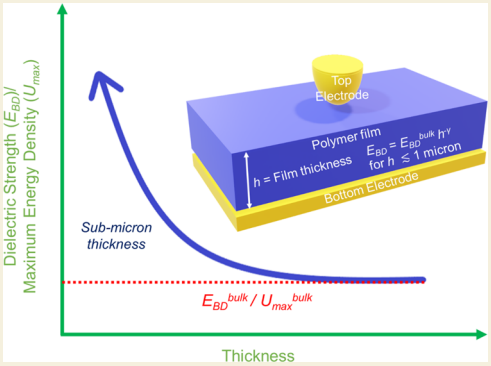

KEYWORDS: *thin polymer films, capacitive energy density, dielectric breakdown strength, dielectric capacitors, glass formation, chain entanglement, yield, aging, nanocapacitors*

INTRODUCTION

The growing need for sustainable energy storage devices demands innovation in materials and processes used for energy storage applications.[1,2] One of the key challenges for energy storage devices is to simultaneously increase the energy and power density of these devices for next-generation applications.[1,2] Dielectric capacitors[3] have the potential to offer the higher power (ultrafast rate of charge/discharge) densities required for advanced applications, as compared to their electrochemical counterparts such as batteries, supercapacitors, and fuel cells,[4−6] but present-day dielectric capacitors have significantly lower energy densities (limiting total energy capacity) than electrochemical energy storage devices.[2,7] To meet future manufacturing requirements, there is an urgent need to enhance the energy density of dielectric capacitors for high-power density applications.[8,9]

The recoverable energy density (U_d) in a dielectric material is defined as,

$$U_d = \int_{D_r}^{D_{max}} E \, dD \tag{1}$$

where D_{max} is the maximum electric displacement, D_r is the residual electric displacement, E is the electric field and D is the electric displacement. Dielectric materials can be divided into linear, paraelectric, ferroelectric, relaxor ferroelectric, and antiferroelectric,[10−12] depending on the relationship between the electric displacement and field. D_{max} is dictated by the dielectric strength E_{BD} of the material. For linear dielectrics, the maximum energy stored (U_{max}) in the electric material is proportional to the square of dielectric strength,[13] i.e., $U_{max} \propto E_{BD}^2$. Evidently, enhancing the E_{BD} of the dielectric material

Received: September 10, 2024
Revised: October 31, 2024
Accepted: November 27, 2024
Published: December 13, 2024

https://doi.org/10.1021/jacsau.4c00833
JACS Au 2025, 5, 121−135

provides a route for enhancing the energy density of materials. Dielectric capacitors can have ceramics or dielectric polymers as dielectric media.[2] Polymeric materials have the advantages of flexibility, self-healing nature, progressive or "graceful" failure, easy processability, roll-to-roll fabrication, high dielectric strength, and low loss tangent.[11] In contrast, ceramics have higher permittivity, low dielectric strength, and a higher loss. Although ferroelectric dielectrics (polymers or ceramics) have higher permittivities, and thus higher D_{max}, as compared to linear dielectrics,[14] the energy loss in ferroelectric dielectrics is significantly higher than for linear dielectrics, thus making linear dielectric polymers (such as polypropylene, polycarbonate) materials of choice for industrial-scale applications. Specifically, strategies to improve the energy density[15] of linear dielectric polymers are needed for developing high energy density dielectric capacitors for industrial applications, such as in electric vehicles and flexible electronics.[2]

The miniaturization of electronic and energy storage devices requires ultrathin polymer films with submicron thicknesses as active or passive materials. As a byproduct of this type of material development, film confinement can affect material properties in unique ways and offers opportunities to better understand the behavior of materials at the molecular and atomic scales.[16] For polymers, it has been demonstrated that ultrathin polymer films[17] can give rise to changes in mechanical properties,[18,19] optical properties,[20,21] film density,[20,22] glass transition temperature (T_g),[23] ionic conductivity,[24] and energy absorption[25] as compared to their bulk counterparts. Some of these property changes might be accounted for by the presence of the mobile layer near the surface of the glass-forming polymers.[26] Exploring how dielectric energy storage properties change from that of bulk polymers to those in thin (≈μm) and ultrathin (≈nm) polymer films, i.e., "finite-size" effects, is of importance from scientific as well as technological standpoints. Additionally, studying the interaction of the electric field with polymers by changing the film thickness can provide unique insights into polymer properties under an electric field. More broadly, such size-dependent dielectric behavior is also relevant to understanding the behavior of cell membranes[27] and electrical injury[28] under electric fields. More generally, finite-size effect on dielectric properties of materials is a ubiquitous phenomenon. For instance, the permittivity of water decreases by as much as 16-fold from bulk to 5 nm thick films due to loss of rotational entropy,[29] results which extend to fluids in general.[30]

Regarding the influence of film thickness h on dielectric strength, it has been generally observed that inorganic dielectrics generally follow an inverse power-law dependence of dielectric strength on the film thickness, which can be rationalized by an increased uniformity in thinner films and the presence of fewer defects.[31,32] However, for polymer films, the dielectric strength vs h relationship is not fully understood.[31] It has been shown that the dielectric strength of polymers such as poly(tetrafluoroethylene), poly(methyl methacrylate), polyethylene, etc. can increase by 100% in the range of ≈76 to ≈8 μm, and 20 to 30% on decreasing h from ≈2 to ≈0.5 mm (500 μm).[31] However, decreased dielectric strength[33] for metal-coated spin-cast polymer films thinner than 5 μm, and increased dielectric strength[34] in films with no metal coating, have both been observed as a function of h, further complicating the interpretation of dielectric breakdown observations in thin polymer films.[35] The diffusion of metal atoms into the polymer film,[36,37] along with altering the mobile layer properties on metal deposition, might also contribute to some of these discrepancies.

In the present work, we observe that the dielectric strength of entangled glassy polymers increases sharply for films thinner than ≈1 μm thickness, which can be described by a universal power-law relationship. We test the generality of this dielectric strength enhancement by testing the dielectric strengths of a multitude of glassy polymers, poly(methyl methacrylate) (PMMA), polystyrene (PS), poly(2 vinylpyridine) (P2VP), polyimide (PI), and polysulfone (PSU), for a range of molecular masses and a range of film thickness, h values. In contrast to entangled glassy polymer films exhibiting high dielectric strength enhancement, unentangled glassy polymer films, as well as semi-crystalline polymers at room temperature, exhibit only a moderate enhancement of the dielectric strength when the films are made correspondingly thin. Notably, Sabuni and Nelson[38] have shown that the dielectric strength of polymer films drops sharply above T_g. We also observe this trend in our thinner films, but we additionally observe a sharp increase in the dielectric strength for a range of common polymers when the films are in the "ultrathin" film thickness regime.

The dielectric breakdown process can be electronic, thermal, or mechanical in nature.[39] For polymers, the mechanical dielectric breakdown is more common at room temperature or higher temperatures.[39] For mechanical breakdown, the extent of polymer deformation under the applied electric field and the resulting mechanical properties of the films are expected to have predominant significance in controlling the dielectric strength. We base this expectation on the theoretical prediction that solid films become unstable to macroscopic deformation through the application of sufficiently large electric fields where the critical field strength for this type of instability depends on the stiffness of the material[40] and the general tendency for the stiffness of glassy polymer materials to become small in the vicinity of the glass transition. Of course, defect-mediated nucleation can be expected to also be a contributing factor for the dielectric breakdown in some films. As part of this work, we demonstrate that the polymer films deform significantly under an electric field, with deformations ranging up to ≈50%, reaching deep into the plastic regime. Such large plastic deformations under an electric field for glassy polymers have actually been observed previously by Baer and Zhu groups as well[41,42] and we show that this mechanical instability accompanies the film dielectric breakdown in our measurements. Thus, understating the dielectric strength and hence the energy density of the polymer films as a function of film thickness requires the comprehension of the mechanical properties of polymer films as a function of thickness and the extent of deformation. Notably, studies on the mechanical properties of glassy polymer films in the elastic regime (strain ≲2 to 3%) show almost no change from bulk to thin film regime.[18,19] However, for glassy polymer films undergoing large strains well into the plastic regime (strains >5%), "stiffening" of polymer films with decreasing film thicknesses has been observed.[43] These deformation measurements involve relatively large-scale deformations of the films, where one might note the scale of these in the center of the circular membranes and that the stiffening reported is consistent with the macroscopic deformation of ductile amorphous polymer materials in their glass state,[44] but is not generally observed in the stiffness of glassy polymer films in the regime of small deformation. McKenna and co-workers[45] attribute the

https://doi.org/10.1021/jacsau.4c00833
JACS Au 2025, 5, 121−135

stiffening modulus in entangled glassy polymer films to be a "rubbery modulus", as in the case of large deformation measurements on ductile bulk polymer glass materials just mentioned, but in both cases, the reported moduli are far too large in relation to conventional rubbery materials and too small in relation to moduli of polymer glass materials in the linear elasticity regime. Such anomalously large moduli values are also observed in creep measurements on amorphous polymer materials in the glass state where large-scale deformations are involved.[46] Moreover, the degree of stiffening in the highly entangled polymer glass films is much higher than unentangled polymer films in their glass state that tend to be very brittle[47,48] appears to be strongly dependent on the fragility of glass formation, pointing to some connection of this remarkable stiffening phenomenon to the glass-forming nature of the films rather than to the elasticity of rubbery materials. We thus question the designation of these apparent moduli as being "rubbery moduli". The large deformation moduli of ductile polymer materials in their glass state involve a convolution of glassy dynamics and the dynamics of polymer entanglement that is currently not well understood theoretically, but this general phenomenon has been exhibited in numerous prior measurements.

Xu et al.[49] have recently offered an explanation of this anomalous elasticity of polymer materials in their glass state under large deformation conditions as arising from fluctuations in the local stiffness inherent to polymers in their glass state acting in concert with the entanglement network stabilizing this dense network of physical bonds. It is natural in this proposed model of the large-scale deformation of highly entangled polymers in their glass state that the apparent moduli should be intermediate to polymer glasses and rubbery materials observed under linear elasticity deformation conditions, and for the moduli to be greatly influenced by the fragility of glass-formation, as this property of glass-forming liquids is highly correlated to the elastic heterogeneity of polymer material in its glass state. It is also understandable why this nonlinear stiffening effect tends to disappear above T_g where the physical cross-links "melt",[50] leading to the loss of the high dielectric strength of thin polymer films of this kind.[38]

By invoking the concept that dielectric breakdown involves inducing macroscopic mechanical deformations of the film by the applied E-field, the documented phenomena of stiffening properties of ultrathin films can explain their enhanced dielectric breakdown strength. There are other studies corroborating the enhancement of the effective film stiffness of ultrathin entangled polymer films with reducing film thickness. Simulations of the specific penetration energy (a measure of impact strength) of ultrathin polymer films with respect to ballistic penetration indicate that this quantity increases as power-law with decreasing h in the ultrathin film regime,[51] while the penetration energy itself increases monotonically and roughly linearly with h. Projectile impact measurements[52] on model amorphous polymer materials (polystyrene, polycarbonate) have further indicated a precipitous drop in the impact resistance near T_g, similar to the observations of Sabuni and Nelson[38] and others for the dielectric strength. The parallelism between these film "strength" parameters subject to strong electric and deformation fields, respectively, is striking, and we observe exactly this same type of power-law scaling for the dielectric strength of thin polymer films. Below, we develop this idea further to understand the effect of chain entanglement on film dielectric strength. Finally, we note there have been recent general theoretical arguments for a "stiffening" of the high-frequency modulus in highly confined liquids.[53,54]

One of the many complicating factors that can influence the properties of our cast polymer films is that a skin layer near the free boundary of the evaporating film can form as it is drying leading in some cases to due to a significant enrichment of the polymer in the interfacial region as the film dries, a phenomenon suggested theoretically by de Gennes[55] and studied by molecular dynamics simulation.[56] This inherently non-equilibrium phenomenon could conceivably influence the dielectric breakdown of the films and make this property sensitive to exactly how the films are made. Accordingly, we carefully checked how film annealing above T_g, after their casting influenced their dielectric breakdown strength, and found that annealing reduced their relative dielectric breakdown strength compared to cast films, however, the enhancement trends remained the same. This phenomenon, which is evidently of practical importance in relation to device fabrication based on this type of polymer film formation process, prompted us to perform additional measurements to better understand why film processing history could have such a great impact on the dielectric breakdown strength. Further measurements indicated that this nonequilibrium phenomenon could be traced to the large deformation behavior of glassy polymer films induced by large electric fields. This this kind of processing history effect is well-known to influence polymer mechanical properties in a significant way. We believe that properties related to the large deformation of the polymer films as being prevalent in understanding and controlling dielectric strength, and we adopt this as our working model in our discussion below.

To check potential changes in "free volume" influencing the observed trends with decreasing film thickness in the dielectric strength of our polymer films below ≈1 μm, we estimated the density change with the thickness of polystyrene (PS) films using ellipsometry. These measurements clearly indicated that density changes in the submicron thickness are negligible until the thicknesses reach ≈100 nm, and thus the observed range of enhanced breakdown strength simply does not correlate with film density change. On the other hand, the observed enhancements of dielectric strength do seem to be comparable to observed changes in the permittivity of confined water[29] and other polar fluids,[30] which might be relevant to understanding the origin of the critical scale on the order of 1 μm at which significant deviations from the bulk dielectric strength first emerges.

In order to assess the potential utility of these thin films for applications, we fabricated polymeric nanocapacitors from solvent-cast PMMA films and observed that these nanocapacitors exhibit an ultrahigh discharge energy density (U_d) as large as 27 J/cm^3 and an efficiency (η) larger than 80% at a maximum electric field of 1438 V/μm. The efficiency of the nanocapacitor remains higher than 80% for the applied electric field values in the range between 0 to E_{BD}. These discharge energy densities and efficiencies are much higher than those of competing ferroelectric materials, so the thin and ultrathin thickness regimes of glassy entangled polymer films are indeed highly promising for device applications.

https://doi.org/10.1021/jacsau.4c00833
JACS Au 2025, 5, 121−135

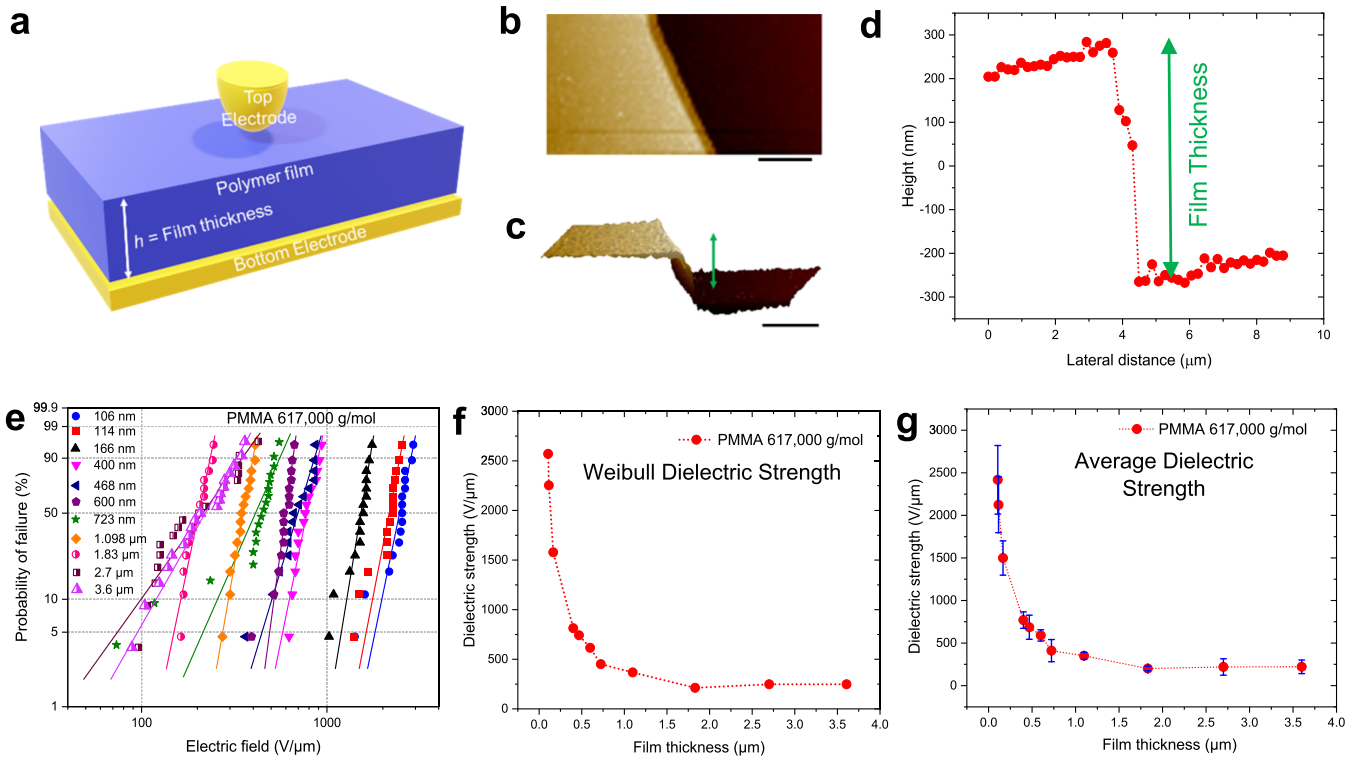

Figure 1. Power-law increase in the dielectric strength in ultrathin films (a) Schematic showing measurement of dielectric strength of thin polymer films (thickness h) between two electrodes. (b) Atomic force microscopy (AFM) image showing the scratch test-based procedure for precise measurement of the film thickness of polymer films supported on bottom electrodes (aluminum on silicon). (c) 3D AFM image of scratched polymer film showing the film height. The scale bar corresponds to 3 μm in both (b, c). (d) Quantitative measurement of polymer film thickness h from AFM images shown in (b) and (c). (e) Weibull probability plots for the dielectric strength of poly(methyl methacrylate) (PMMA 617 000 g/mol) for different h. (f) Weibull dielectric strength (at 63.2% probability of failure) as a function of h. (g) Average (arithmetic mean) dielectric strength with error bars as a function of h.

RESULTS AND DISCUSSION

Anomalously High Dielectric Strength in Thin Entangled Glassy Polymer Films

Figure 1a shows a schematic describing our dielectric testing methodology on thin polymer films. The films were flow coated on aluminum-coated silicon wafers and testing was performed by connecting a spring-loaded ball electrode to the top surface of the film and by connecting the bottom electrode to the ground. The polymer film thickness was varied by changing the polymer solution concentration and flow-coating speed to study film with h in the range of ≈100 nm to a few μm. To precisely measure h, as required for dielectric strength estimates, we utilized the atomic force microscopy (AFM) scratch test and thin film interferometry (on reference silicon wafers). Briefly, the polymer films were scratched with a sharp knife or tweezer such that the polymer came off at the scratched location without damaging the electrode and substrate underneath. Figure 1b shows the representative 2D AFM image of polystyrene film scratched in order to make a thickness measurement. A 3D representation of the same image is shown in Figure 1c demonstrating the height of the polymer film (with the double-headed arrow). The height of the polymer film is measured by analyzing the line profile across the AFM scratch images. Figure 1d shows the line profile of images Figure 1b,c showing a height of ≈525 nm. The precise measurement of height is crucial for calculating the dielectric strength of thin polymer films (h < 1 μm).

Figure 1e shows the Weibull failure plots of different h of PMMA having 617 000 g/mol molecular mass as a function of the electric field. The Weibull dielectric strengths parameters are calculated using the two-parameter Weibull function[2]

$$P(E) = 1 - \exp[-(E/E_{BD})^{\beta}] \quad (2)$$

where $P(E)$ is the probability of dielectric failure, E is the measured dielectric strength, E_{BD} is the Weibull dielectric strength at 63.2% probability of failure, and β is the Weibull "shape parameter". The spring-loaded top electrode (for point contact as well as wire loop contact) is contacted softly to the top of the film; see Supporting Information (SI) Figures S1 and S23. The probability of dielectric failure at a particular electric field decreases as h decreases. In particular, we studied the dielectric strength for 13 films having different h and a fixed molecular mass where we observe a progressive increase in the dielectric strength as h is reduced in magnitude. The individual dielectric failure plots are attached in SI Figure S4a–k where the breakdown voltage itself increases with h.

The Weibull dielectric strength, measured at the 63.2% probability of failure using Weibull analysis, is shown in Figure 1f. The dielectric strength starts to increase above the bulk dielectric strengths when h decreases below ≈1.5 μm. Furthermore, the ultrathin films with h < 0.5 um show a sharp increase in the dielectric strength as h decreases. In addition to Weibull dielectric strength, the average dielectric strength along with the standard deviation error bars is shown in Figure 1g. The average dielectric strength also follows the same trend as Weibull dielectric strength as expected. This

https://doi.org/10.1021/jacsau.4c00833
JACS Au 2025, 5, 121−135

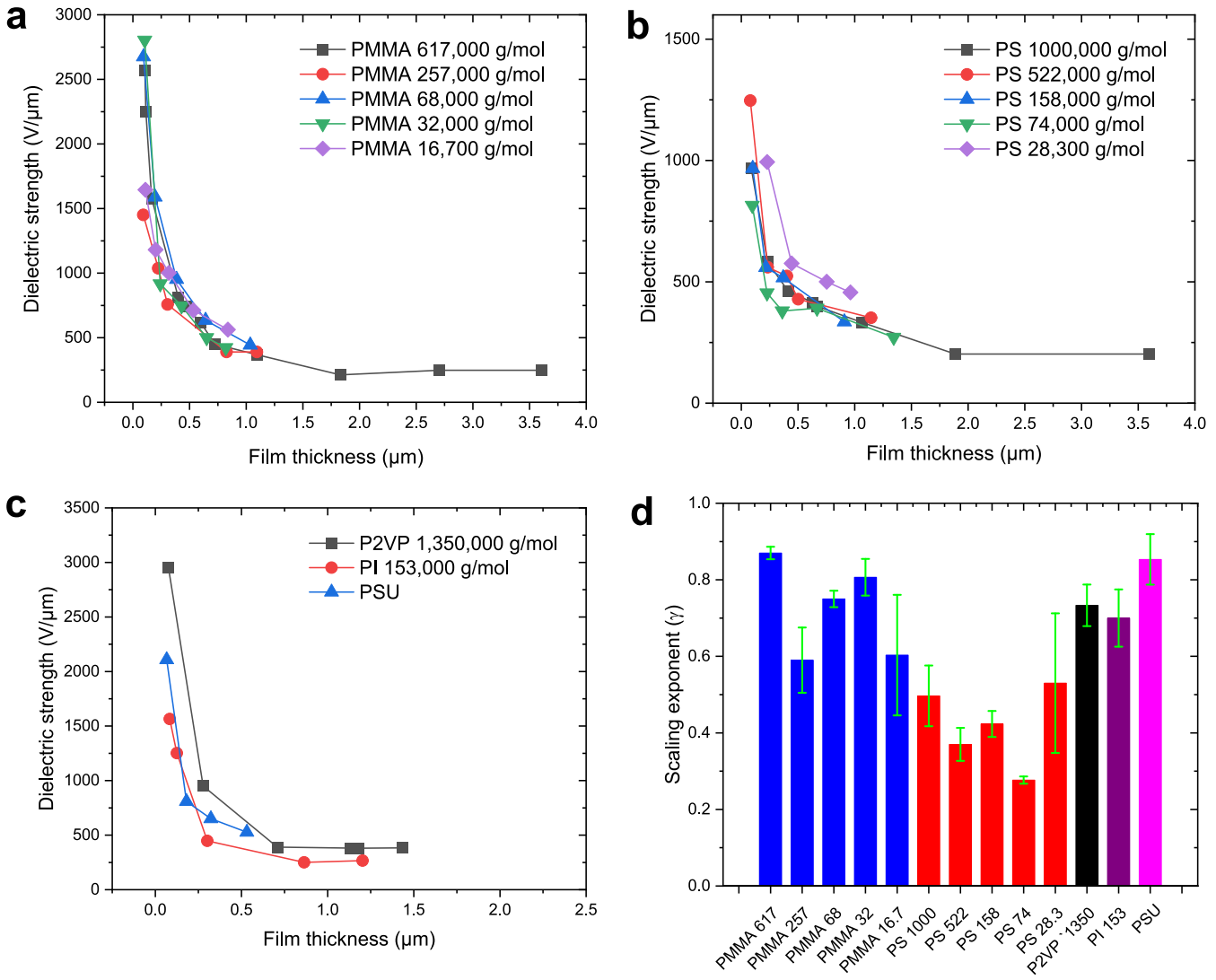

Figure 2. Universality of the exponential increase of dielectric strength (E_{BD}) in ultrathin entangled glassy polymers. (a) The Weibull dielectric strength of different molecular masses (above entanglement molecular mass of the bulk material) of poly(methyl methacrylate) PMMA as a function of film thickness (h) for ultrathin films showing a universal trend for a power-law increase of the dielectric strength. (b) The Weibull dielectric strength of different molecular mass polymers (above the entanglement molecular mass) of polystyrene (PS) as a function of h showing a universal power-law increase in dielectric strength as a function of h for ultrathin films. (c) The power-law increase of Weibull dielectric strength as a function of h for poly(2-vinylpyridine) (P2VP), polyimide (PI), and polysulfone (PSU) in ultrathin film regime. The arithmetic average dielectric strength along with error bars for PMMA different molecular weights is shown in SI Figure S8(f), for different molecular weights PS is shown in SI Figure S14(e), and for P2VP, PI, and PSU is shown in SI Figure S18(f). (d) The scaling exponents (γ) for different polymers as calculated from $E_{BD} \propto h^{-\gamma}$.

sharp increase in dielectric strength offers a high potential for designing ultrahigh energy density materials.

These changes in the dielectric strength parallel other property changes in ultrathin polymer films including changes in T_g,[23] film density,[20,22] optical properties,[20,21] ionic conductivity,[24] mechanical properties such as Young's modulus,[18,34] and cell adhesion.[57] However, these property changes only become substantial in the sub-100 nm regime. Notably, few studies have reported the increase in the glassy modulus of polymer films in this ultrathin thickness range.[58,59]

In the case of dielectric strength, we observe a sharp increase in dielectric strength for sub-500 nm films so the onset scale for the property changes is qualitatively larger than normally observed for other properties of thin films. These measurements are reminiscent of the decrease of water permittivity, which starts to manifest in submicron water layer thicknesses.[29]

To gain insight into the mechanism of dielectric failure, we examined the extent of deformation of polymer films under an electric field up to the point of dielectric breakdown. Figure S28 (SI) shows the deformation of PMMA (68 kg/mol) polymer films (500 nm) under an electric field of 200 MV/m (before dielectric failure) (a) AFM image and (b) height profile across the AFM image. The deformation in the polymer film is of the order of ≈50% relative to the film thickness. This demonstrates that the polymer deformation under the applied electric field is well into the plastic regime. We interpret this previously observed stiffening effect of entangled glassy polymer films[43,44,46] to be the primary cause of the large enhancement of the dielectric strength of these films.

https://doi.org/10.1021/jacsau.4c00833
JACS Au 2025, 5, 121−135

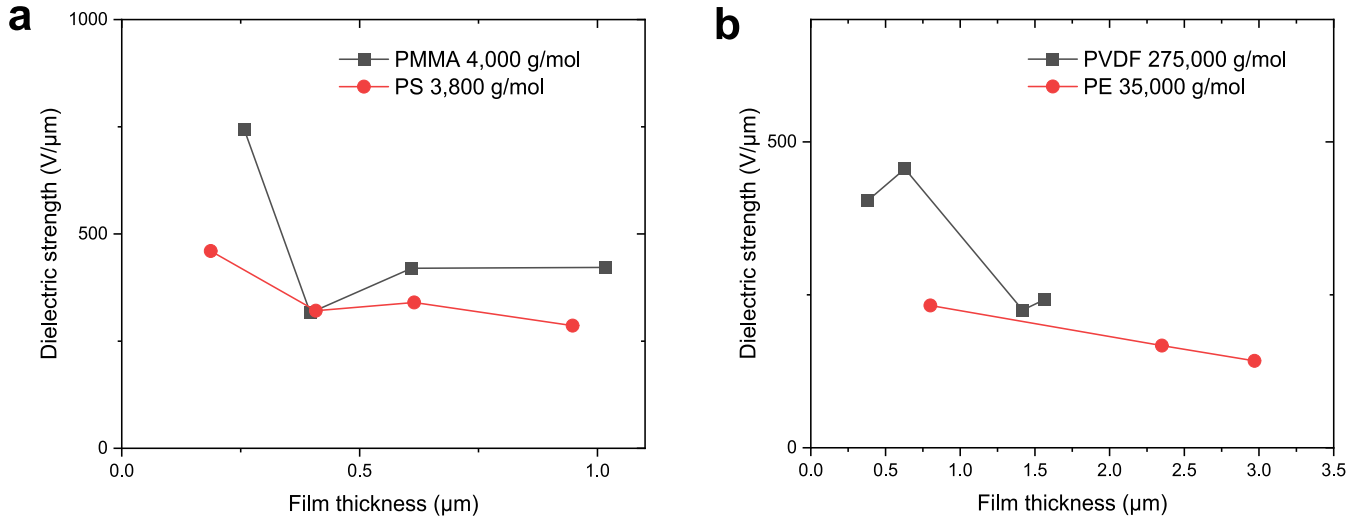

Figure 3. Moderate increase in the dielectric strength (E_{BD}) as a function of film thickness (h) for unentangled glassy polymers and polymer with T_g below room temperature (a) The Weibull dielectric strength of poly(methyl methacrylate) (PMMA) (4 kg/mol) and polystyrene (PS) (3.8 kg/mol) as a function of h. The average dielectric strength along with error bars for PMMA 4 kg/mol and PS 3.8 kg/mol are shown in SI Figure S20(e). (b) The Weibull dielectric strength of polyethylene (PE) (35 kg/mol) and poly(vinylidene fluoride) (PVDF) (275 kg/mol) as a function of h. The average dielectric strength along with error bars for PVDF and PE are shown in SI Figure S22(e). The unentangled glassy, as well as semicrystalline polymers, show a relatively moderate increase of dielectric strength as a function of h.

Universality of Dielectric Strength Enhancement for Entangled Glassy Polymer Films

Next, we study the dielectric strength as a function of film thickness for different molecular masses of PMMA (entanglement molecular mass, $M_e \approx 10\,000$ g/mol[60]) to further understand the interesting behavior of ultrahigh dielectric strength in ultrathin films. (It should be recognized that the degree of chain entanglement could be altered somewhat by the process of film casting, but we may expect the cast films to be likewise "entangled" if the polymer mass is significantly larger than the entanglement molecular mass of the bulk polymer material under equilibrium conditions, M_e). We observe that the dielectric strength follows a sharp increase as a function of film thicknesses for the molecular mass range of 617 000 to 16 700 g/mol as shown in Figure 2a. Furthermore, the dielectric strength vs film thickness plot appears to follow close to a universal trend for the molecular masses studied. The dielectric failure plots for different film thicknesses for the different molecular masses of PMMA are shown in the SI: Figures S4(a–k), S5(a–e), S6(a–e), S7(a–e), and S8(a–e). The arithmetic average dielectric strength along with error bars for PMMA different molecular weights is shown in SI Figure S8(f) and follows the same general trend, as expected.

To test the universality of the dielectric strength enhancement in entangled polymer films with decreasing h, we study the dielectric strength of different molecular masses of polystyrene (PS) ($M_e \approx 13\,000$ g/mol[60]) dielectric as well. The dielectric strength as a function of h of the different molecular masses of polystyrene is shown in Figure 2b. The polystyrene films also follow a near-universal curve for the increased dielectric strength as a function of decreasing h. The Weibull probability plots for the different molecular masses of PS are shown in SI. The arithmetic average dielectric strength along with error bars for PS different molecular masses is shown in SI Figure S14(e).

Next, we test the dielectric strength of poly(2-vinylpyridine) (P2VP), polyimide (PI), and polysulfone (PSU) as a function of h and we observe that the dielectric strength of these polymers also follows a sharp increase as h decreases as shown in Figure 2c. The Weibull probability plots for the different h of P2VP, PI, and PSU are shown in SI Figures S16(a–f), S17(a–f), and S18(a–f), respectively. The arithmetic average dielectric strength along with error bars for P2VP, PI, and PSU is shown in SI Figure S18(f) To further analyze the trend of increasing dielectric strength, we consider the scaling of the dielectric strength with h,

$$E_{BD} \propto h^{-\gamma} \tag{3}$$

where E_{BD} is the dielectric strength and γ is an empirical scaling exponent quantifying the enhancement of the dielectric strength with decreased thickness. The estimated scaling exponents γ for PMMA, PS, P2VP, PI, and PSU are shown in Figure 2d., i.e., the larger γ, the stronger the increase in dielectric strength. We observe that γ values for different molecular masses of PMMA lie between 0.5 and 0.9 as shown in Figure 2d. These apparent exponents are evidently higher than those observed for the h dependence dielectric strength of thicker polymer films reported in the literature.[31] The dielectric strength of ultrathin film PMMA (257 000 g/mol) stays high until its glass transition temperature (T_g) and decreases for T above T_g (122 V/μm at 150 °C, as shown in SI Figure S24). The exponent values for PS dielectric strength range from 0.25 to 0.6, and are thus lower than those observed for PMMA. The exponent γ values for P2VP, PI, and PSU are close to $\gamma \approx 0.8$, as shown in Figure 2d.

Dielectric Strength of Unentangled Glassy and Semi-Crystalline Polymer Films

In Figure 2, we showed the dielectric strengths of entangled glassy polymers as a function of film thickness. Next, we look at the dielectric strength of PS and PMMA at molecular masses much lower than the bulk entanglement molecular mass as a function of h. We used PMMA 4000 and PS 3800 g/mol for this study. The dielectric strength of PMMA 4000 and 3800 g/mol as a function of h are shown in Figure 3a. The Weibull probability failure plots for the individual thicknesses of PMMA 4000 g/mol and PS 3800 g/mol are shown in

https://doi.org/10.1021/jacsau.4c00833
JACS Au 2025, 5, 121–135

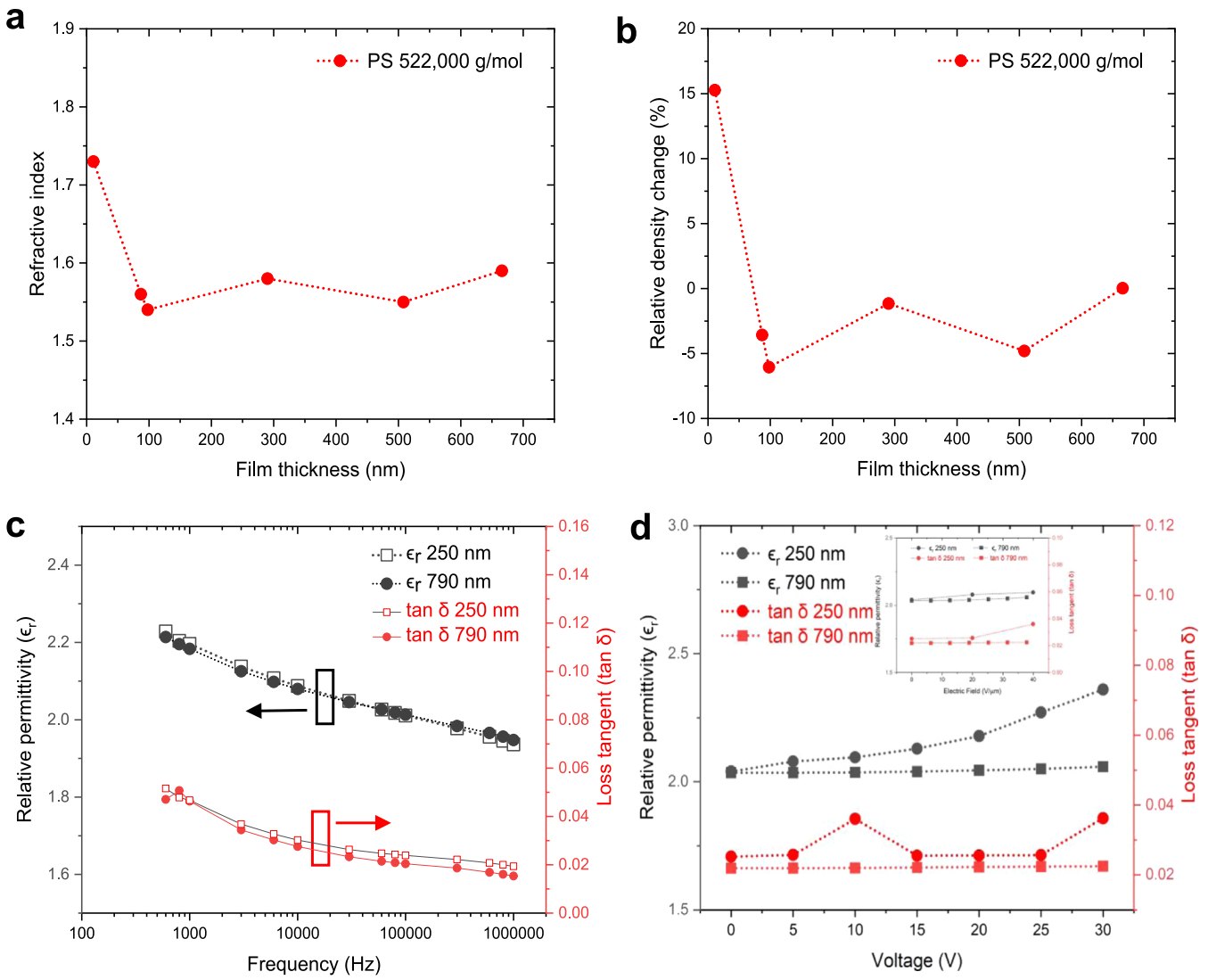

Figure 4. Refractive index, density, and permittivity as a function of film thickness h. (a) Refractive index as a function of h. (b) The calculated "density change" as a function of h. The density change is observable for h smaller than 100 nm, while the dielectric strength starts to increase below $h \approx 1$ to 1.5 μm (c) The effect of h on relative permittivity (ε_r) and the loss tangent (tan δ) as a function of frequency for films with different h (i.e., 250 and 790 nm), showing similar relative permittivity and slightly enhanced loss tangent for the thinner film at higher frequencies (d) The relative permittivity (ε_r) and the loss tangent (tan δ) at high voltage showing enhanced permittivity for the thinner film at higher voltages at 50 kHz. Inset: Relative permittivity (ε_r) and the loss tangent (tan δ) as a function of the electric field for the films.

Supporting Information Figures S19(a–d) and S20(a–d) respectively. The average dielectric strength along with error bars for PMMA 4 kg/mol and PS 3.8 kg/mol are shown in SI Figure S20(e). Although the dielectric strength increases for the low molecular mass PS and PMMA, the increases are not as sharp as that observed for the entangled glassy polymers. This suggests that the higher mobility in these films might facilitate the dielectric breakdown of these relatively low molecular mass unentangled glassy polymers.

We also studied the dielectric strength of unentangled polymer films having a T_g below room temperature, in order to compare the dielectric strength with that of entangled glassy polymers. Figure 3b shows the dielectric strength of poly(vinylidene fluoride) (PVDF) and polyethylene (PE) as a function of film thickness. The individual Weibull probability plots for PE and PVDF are shown in Supporting Information; see Figures S21(a–c) and S22(a–d). The average dielectric strength along with error bars for PVDF and PE are shown in SI Figure S22(e). The dielectric strengths of PVDF and PE show only a moderate increase of the dielectric strength as a function of decreasing h, as opposed to the sharp increase observed in the entangled glassy polymer films, as discussed further below.

A small densification of the polymer films in the ultrathin film thickness regime (see Density and Permittivity Measurements section), an effect perhaps due to the segregation to the interfacial region of the film and other mechanisms for reliving packing frustration in the thin films, might explain the modest enhancement of the dielectric breakdown strength in these films. This atomic-scale mechanism of the breakdown strength remains speculative, however, and here we simply note that the magnitude of this effect is evidently rather small in the thin unentangled polymer films.

Density and Permittivity Measurements

To further probe the origin of the dielectric strength enhancement upon reducing h, we study the density of

https://doi.org/10.1021/jacsau.4c00833
JACS Au 2025, 5, 121–135

polystyrene films as a function of h. In order to estimate the density of ultrathin polymer films, we measured the refractive index of the substrate-supported polystyrene films as shown in Figure 4a. We observed that the refractive index n increases for ultrathin films with h < 100 nm. The density of the films is calculated using the Lorentz−Lorenz equation,

$$\frac{n^2 - 1}{n^2 + 1} = \frac{\alpha N_A}{3\varepsilon_0 M_0}\rho \quad (4)$$

where n is the refractive index, ρ is the mass density, α is the molecular polarizability of the monomer repeat unit, N_A is Avogadro's number, ε_0 is the permittivity of free space and M_0 is the monomer repeat unit molecular mass. The estimated film density evidently increases somewhat as h decreases below 100 nm, as shown in Figure 4b. Although a detectable density increase is observed in the ultrathin thickness regime, the dielectric strength enhancement starts to become significant and occurs on a larger thickness on the order of 1 μm. It has been previously reported that the density of PMMA films increases somewhat with decreasing h and decreases for PS films with decreasing h.[61] Notably, Roth and co-workers reported an increase in density for both PMMA and PS as h decreases,[21] but the origin of this difference is not evident to us. We then conclude that while density changes apparently occur in ultrathin films, these changes are probably only a small contributing factor influencing the dielectric strength of our ultrathin polymer films. Moreover, we expect the quantitative density enhancement in thin films to be smaller than the values that we estimate from the Lorentz−Lorenz equation because this bulk continuum theory can be expected to "break down" at a quantitative level in the ultrathin film regime.[22] Nonetheless, we expect that the finding of a relative density enhancement in our thin polymer films is a real effect.

Apart from the dielectric strength, the dielectric permittivity is another major component of the interaction of the electric field with polymer films. Since the capacitive energy density (U) can be expected to vary nearly linearly with the polymer film permittivity, we study the effect of varying h on the polymer film permittivity. We utilize liquid metal (Eutectic Gallium Indium alloy)-coated electrodes for measuring the film permittivities, as opposed to the use of soft point contacts as in the case of the dielectric strength measurements. Figure 4c shows our measured estimates of the dielectric permittivity of two PMMA 257 kg/mol films having two h (250 and 790 nm). The dielectric permittivities of these polymer films are nearly equal, showing that the dipole polarization is relatively independent of h, in contrast to the film dielectric strength. Figure 4d shows the apparent dielectric constant of different h as a function of increased voltage (at higher electric fields). The thinner film shows a slightly higher loss as compared to the thicker film. Interestingly, the dielectric permittivity of the thinner film increases slightly as a function of applied voltage. The enhanced permittivity of thinner films at similar voltages might be due to the nonlinear effects observed by films at high electric fields, as demonstrated by Daiham et al., given that the thinner films undergo higher electric fields as compared to the thicker ones at the same voltage. Notably, thinner films tend to show a higher loss tangent ($\tan\delta$) as a function of frequency as well as voltage on account of higher leakage current.

Effect of Thermal Annealing on Dielectric Strength of Thin Entangled Glassy Polymer Films

One of the ramifications of the idea that dielectric breakdown can be viewed as a kind of "yielding" phenomenon arising from film deformation caused by the applied electric field is that physical and molecular factors influencing the mechanical yielding of polymer materials should be germane to understanding the phenomenon of dielectric breakdown. Apart from the dramatic reduction of the dielectric and mechanical strength as quantified by the "yield strength", which is normally proportional to the glassy shear modulus[62−64] G_g, of polymer and other glass-forming materials in their low-temperature glass state, it is often found that the mechanical yield properties of non-crystalline polymer materials can be highly sensitive to the cooling history and the properties of these materials evolve over time,[44,50] a phenomenon referred to as "physical aging". It is then natural to consider whether the dielectric strength and other dielectric properties of our thin films exhibit such "history effects". It is also noted in this connection that these history effects and the brittleness of polymer materials in the glass state are characteristically highly sensitive to the non-linear elastic properties of the material rather than just the material stiffness under small deformation conditions. Deformed glassy polymer materials exhibit a strong propensity to strain softening and associated shear banding and crazing at moderate deformation that can lead to brittle fracture unless the material starts to exhibit strain stiffening which acts to suppress these unstable modes of polymer material deformation that follow yield.[44,50,65] Notably, the large deformation properties of different polymer materials can be highly polymer-specific. For example, polystyrene in the glass state tends to be a brittle material that readily forms shear bands, crazes, and cracks[66−70] because of the large strain softening and highly limited strain-stiffening exhibited in this material after a long period of aging, while polycarbonate tends to be "tough" material because of the limited strain softening and relatively large strain stiffening that sustains large scale material deformation without material rupture.[44,50,65]

Polystyrene materials can be transformed into tough materials similar to polycarbonate materials by rapidly quenching these materials into the quenched state and not waiting a long time to allow the material to "relax" or by "prestressing" the material to "rejuvenate" the material after a long period of aging into a material stare that behaves more like the freshly quenched glass material. Huge efforts have been made to understand this rich behavior of the large deformation of polymer glasses, but the current level of understanding is fairly qualitative.[71,72] One phenomenological trend that is highly relevant to the current study is that chain entanglement, and thus polymer mass, can greatly influence the magnitude of the strain stiffening of non-crystalline materials, along with temperature, and this effect can have a large effect on the ultimate toughness of this class of materials.[44,50,71−75] The possibility that film casting also influences chain entanglement and aging associated with the evolution of entanglement in time as the film slowly evolves to an equilibrium state is a further complication that might arise in cast ultra-thin films. Based on our view of dielectric breakdown strength as a corresponding field-induced counterpart of mechanical deformation, we may likewise anticipate that chain entanglement greatly enhances dielectric breakdown strength in comparison to unentangled polymer materials. In the present section, we show that aging effects (accelerated aging by thermal

https://doi.org/10.1021/jacsau.4c00833
JACS Au 2025, 5, 121−135

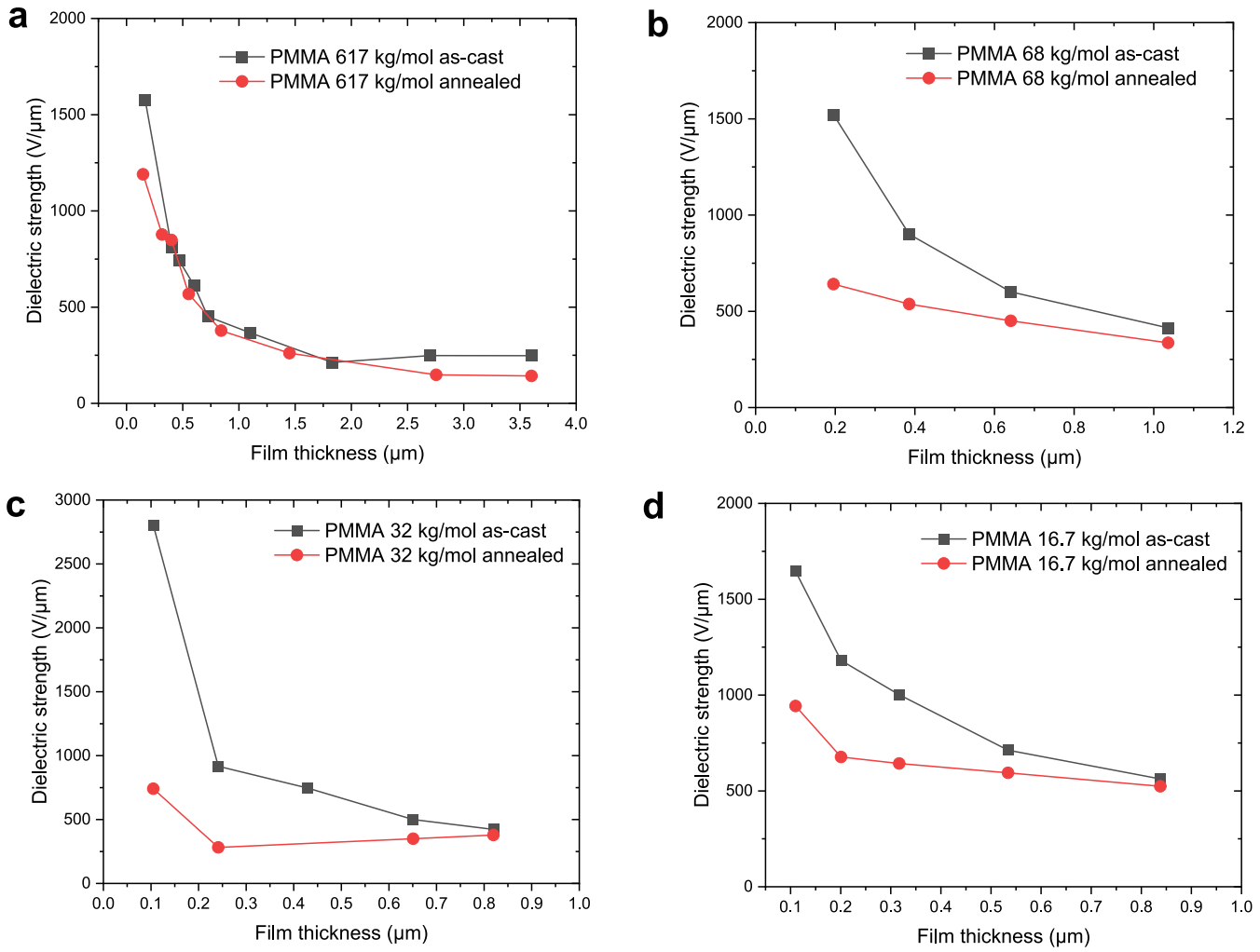

Figure 5. Effect of annealing on the dielectric strength of ultrathin entangled glassy polymer films. The Weibull dielectric strength of as-cast and annealed (annealed at $T \approx T_g + 110$ °C for 48 h). (a) PMMA 617 000 g/mol. (b) PMMA 68 000 g/mol. (c) PMMA 32 000 g/mol. (d) PMMA 16 7000 g/mol showing decreased dielectric strength as compared to the as-cast films in the ultrathin film regime. The dielectric strength of the annealed films approaches the dielectric strength of as-cast films for thicker films. The average dielectric strength along with error bars and scaling exponents are shown in SI Figure S27.

annealing) as seen before in mechanical measurements, are indeed prevalent in our polymer cast films, and in the following section, we further confirm our expectation that the breakdown strength of our thin polymer films can be greatly enhanced by chain entanglement.

Figure 5a–d shows the effect of annealing the films for a relatively long period of time on the dielectric strengths of different molecular mass samples of PMMA (annealed at 220 °C for 48 h). Evidently, the dielectric strength for the ultrathin films progressively decreases on annealing as compared to as-cast films and we observe this effect to become more pronounced for "thin" films for which $h < 1$ μm. The difference between the dielectric strength of the as-cast and the annealed films is largest for the thinner films. The dielectric strength of annealed film also increases as h decreases, but the observed increase is smaller compared to as-cast films.

SI Figure S27(e) shows the effective exponents γ (see eq 2) quantifying the increase of dielectric strength as a function of h for the annealed PMMA films, as compared with the as-cast films for the different molecular masses. The γ values of annealed films are lower than their as-cast counterparts. There are clearly significant processing history effects on the properties of the cast thin films which provide additional hints at the origin of dielectric strength enhancement in cast films. The control of this type of property variation and a better understanding of its origin will be essential for utilizing this phenomenon in applications.

Polymeric Nanocapacitor Devices Based on Thin Entangled Glassy Polymer Films

As the ultrathin entangled polymers show high dielectric strength, the capacitors based on ultrathin polymer films should have a higher energy density. However, it is difficult to make polymeric capacitors based on ultrathin polymer films with $h \approx 100$ nm. This is due to the diffusion of metal atoms inside the film during electrode deposition.[36,37] We observe that the polymer films with sputter-coated metal electrodes show much lower dielectric strength, as compared to the uncoated films; see Figure S26 in SI. The metal deposition can damage the crust layer by infiltration, thus resulting in lower dielectric strength. As such, the methods for non-destructive electrode deposition need to be developed for utilizing the high dielectric strength of ultrathin polymer films for developing high-energy density capacitors.

https://doi.org/10.1021/jacsau.4c00833
JACS Au 2025, 5, 121–135

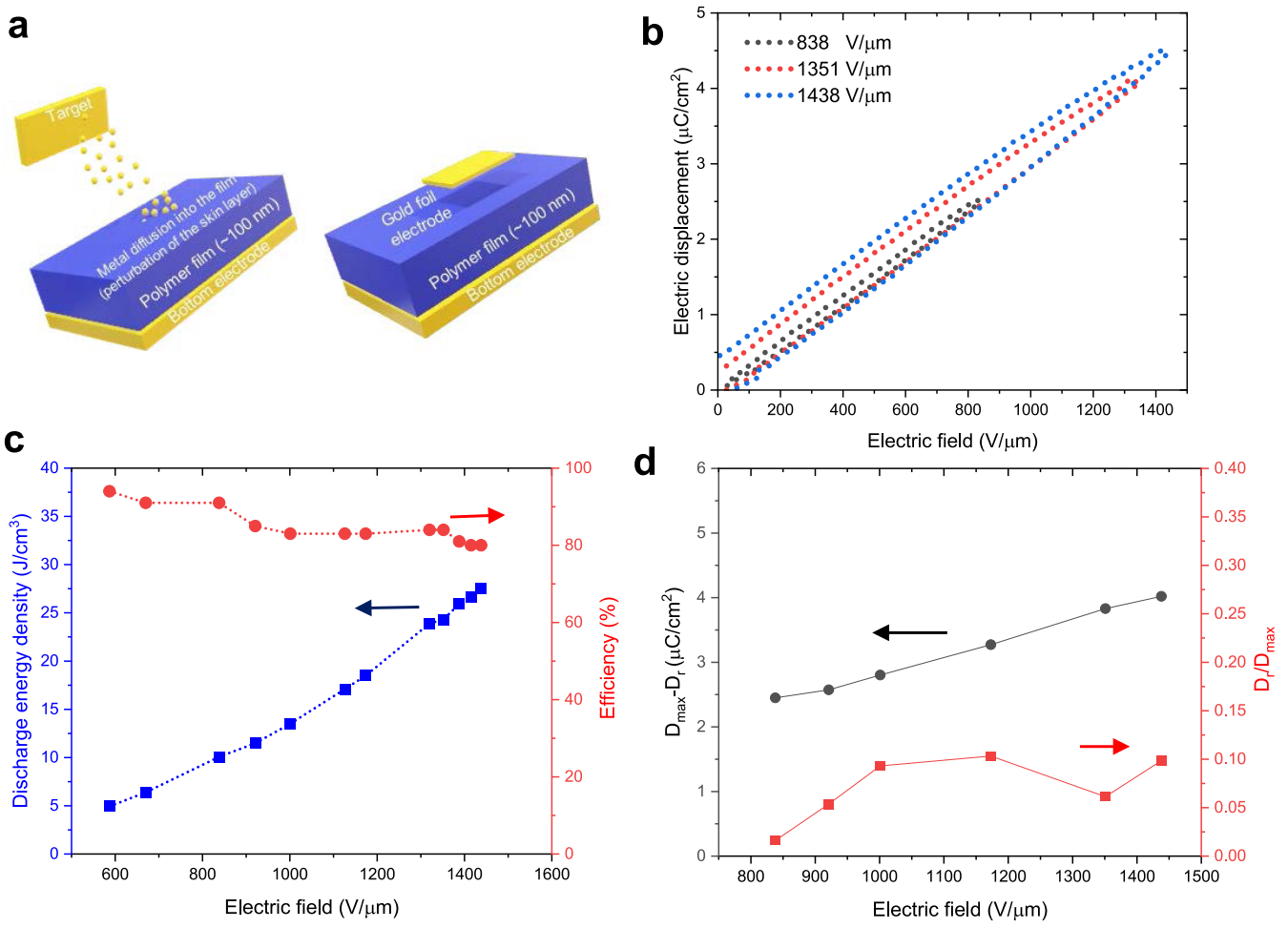

Figure 6. Measurement of energy density in 120 nm thin PMMA polymer films (a) Schematic showing the use of direct gold foil transfer to fabricate electrodes as metal deposition results in diffusion of metal into the thin polymer film. (b) Electric displacement vs field for the thin PMMA film showing linear displacement. (c) Discharge energy density and charge−discharge efficiency vs field showing a maximum energy density of 27.5 J/cm^3 at a field of 1438 V/μm (d) Maximum displacement D_{max} minus residual displacement values D_r and D_r/D_{max} as a function of applied field strength, showing a low residual displacement.

Here, we use a non-destructive method of electrode deposition by floating thin gold foils ($h \approx 100$ nm) on water and picking them up on polymer films. The gold foils are completely sealed by vacuum and have areas in the range of 0.02 to 0.16 mm^2. Figure 6a shows a schematic of the direct fabrication of gold foil electrodes without the need for sputter coating. Figure S25 shows an image of the gold foil electrode on polymer film. Figure 6b shows electric displacement (D) vs electric field for a PMMA (257 kg/mol) polymer film with $h \approx$ 120 nm sandwiched between two electrodes. The maximum displacement is 4.47 μC/cm^2 at an electric field of 1438 V/μm. This field strength is slightly lower than the dielectric strength, which might be due to the AC field or the higher area for measurements. Furthermore, the electric displacement shows a near-linear behavior as a function of the field strength. Figure 6c shows discharge energy density and efficiency vs electric field for the nanocapacitor showing an ultrahigh energy density of 27.5 J/cm^3 at an electric field of 1438 V/ μm with efficiency above 80%. The residual displacement (D_r) remains significantly lower as compared to the maximum displacement D_{max}; see Figure 6d.

Figure 7a shows the comparison of the maximum discharge energy density of polymeric nanocapacitors with the best capacitors available in the literature. This polymeric nanocapacitor shows the highest dielectric strength of any previously developed polymer capacitor. The maximum energy density of the polymeric nanocapacitor is comparable to the ferroelectric nanocomposite capacitors. Notably, ferroelectric polymer-based capacitors have higher losses as compared to linear dielectric capacitors, thus, making linear dielectric polymers the capacitors of choice for any application. Due to the low-loss nature of polypropylene and polycarbonate, they are widely used for capacitor materials as opposed to lossy ferroelectrics. Figure 7b shows a comparison of residual displacement D_r and residual displacement over maximum displacement D_{max} of the polymeric nanocapacitor with other capacitors. The polymer capacitors can deliver high energy at a low loss if the residual displacement is lower. The glassy polymeric nanocapacitor shows the lowest D_r and D_r/D_{max} as compared to other dielectric capacitors, including organic and inorganic dielectric capacitors. The low D_r and D_r/D_{max} values indicate the superior performance of the glassy polymeric nanocapacitor due to its linear nature as compared to the ferroelectric organic or inorganic capacitors. This example demonstrates that linear dielectric glassy nanocapacitors should be the material of choice to minimize loss of energy. A complete comparison of the properties of polymeric nanocapacitors developed in this work with the literature is

https://doi.org/10.1021/jacsau.4c00833
JACS Au 2025, 5, 121−135

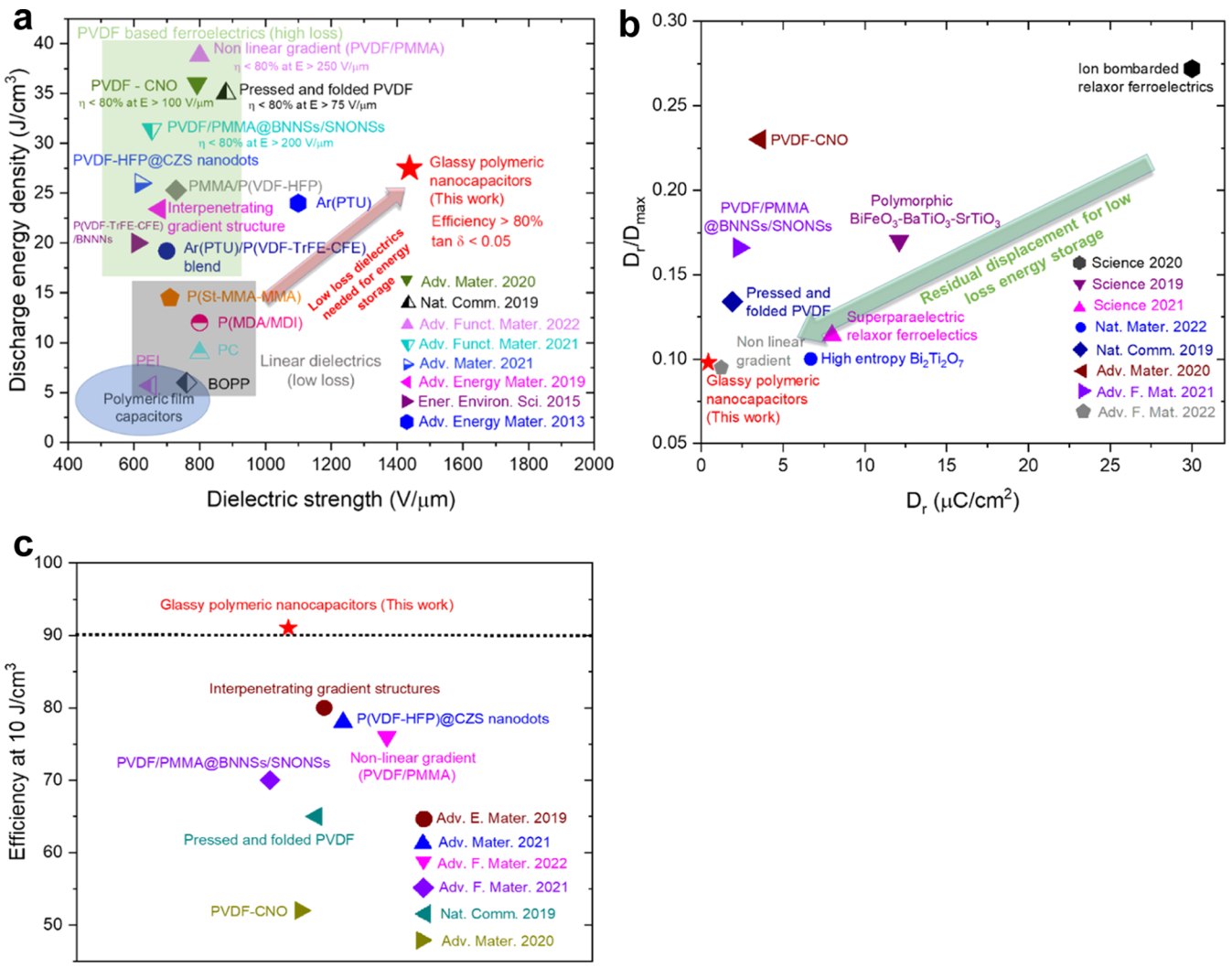

Figure 7. Comparative analysis of the performance of glassy polymeric nanocapacitors with the literature capacitors (a) Comparison of maximum discharge energy density vs field strength showing that glassy polymeric nanocapacitors have the highest energy density among linear capacitors, which are needed for energy storage due to low loss as opposed to the ferroelectric capacitors, which have high loss and are inefficient for energy storage. (b) Comparison of D_r/D_{max} for glassy polymeric nanocapacitors with the best capacitors in the literature showing that D_r/D_{max} is lowest for polymeric nanocapacitors. (c) Comparison of the charge−discharge efficiency of polymeric nanocapacitors with the literature capacitors at a discharge energy density of 10 J/cm^3, showing that the nanocapacitors demonstrate an efficiency higher than 90%, a value that is significantly higher than the competing ferroelectric-based capacitors due to their lossy nature. The list of literature references and the indicated performance values are summarized in SI Tables S1 and S2.

shown in Tables S1 and S2 in SI, along with references describing these results.

Typically, capacitors are used at voltages much lower than the breakdown voltage to maximize the lifetime of capacitors. As an example, BOPP capacitors are used at around 100−200 V/μm, which is 15 to 25% of the breakdown strength of BOPP. Thus, we compare the efficiency of the glassy polymeric nanocapacitors at a discharge energy density of 10 J/cm^3 as shown in Figure 7c. The efficiency of the glassy nanocapacitors is higher than 90% at 10 J/cm^3 while that of the ferroelectric capacitors is below 80%. Developing low-loss and high-efficiency dielectric capacitors has significant implications for the use of capacitive energy storage systems in applications. The high efficiency of linear glassy nanocapacitors makes them the ideal dielectric of choice for developing high-energy density dielectric capacitors.

CONCLUSIONS AND OUTLOOK

We report that ultrathin entangled glassy polymer cast films show a sharp increase in dielectric strength with the decreasing film thickness in the submicron thickness region, which makes them attractive as nanocapacitors for simultaneous high-energy density and high-power density devices with further development. Furthermore, we show that this enhancement is universal in entangled glassy thin polymer films by testing a range of polymer films—PMMA, PS, P2VP, PI, and PS. Notably, low molecular mass untangled glassy polymers, and semicrystalline polymers such as PE and PVDF, with glass transition temperature below room temperature, do not show a sharp increase in dielectric strength. Our working model draws a close parallelism between enhanced mechanical stiffness and toughness reported for thin and ultrathin films in the same range of submicron thickness, and we propose that this prevents the E-field-induced mechanical yielding of the polymer film leading to enhanced dielectric breakdown.

https://doi.org/10.1021/jacsau.4c00833
JACS Au 2025, 5, 121−135

Annealing the films above their T_g results in lowering their breakdown strength, but the trends remain the same with reducing film thickness and require more study. In particular, the large dielectric strength of the entangled polymer films is reminiscent of the large enhancement of the ductility of glassy polymer materials such as a PS when subjected to a pre-stress, an enhancement that is lost upon aging the material for a long time after the press stress treatment or by thermal annealing at temperatures above the glass transition temperature. The observation of the ductility by prestressing in this way is limited to entangled polymer materials, and we likewise only see the large enhancement in our polymer films when the chains are entangled and a loss of the enhancement of most of the enhancement in the ultrathin film regime after long annealing.[61,62,64,65] Factors that influence the glass transition temperature, such as changing the polymer topology from linear to ring polymers,[76] should enhance the relative dielectric strength when the polymer masses are not large because of the shift of the glass transition temperature at which yield becomes prevalent in glassy materials when deformed to a significant degree.[64,65] We also been able to increase the dielectric strength of thin polymer films through the introduction of polymer nanoparticles to increase the mechanical strength of the polymer films.[77,78]

To illustrate the practical potential use of these films, we fabricated polymeric nanocapacitors exhibiting an ultrahigh energy density of 27.5 J/cm^3 and a charge−discharge efficiency higher than 80%. Furthermore, the efficiency of the polymeric nanocapacitors remained higher than 90% up to $U_d \approx 40\%$ of U_d^{max}, which is much higher than those of competing ferroelectric polymers and their composites in the same field strength range. These attributes of ultrathin polymeric nanocapacitors make them attractive for use in practical applications with superior performance with further development, compared to existing commercial and literature capacitors.

MATERIALS AND METHODS

Materials

Poly(methyl methacrylate) (PMMA) with molecular masses (M_w) 16 700 g/mol ($Đ$ = 1.06), 32 000 g/mol ($Đ$ = 1.08), 68 000 g/mol ($Đ$ = 1.28), 257 000 g/mol ($Đ$ = 1.16) and 4000 g/mol ($Đ$ = 1.38) were purchased from Polymer Source Inc. The PMMA 617 000 g/mol ($Đ$ = 1.03) was purchased from Agilent Technologies. Polystyrene (PS) with molecular mass 3800 g/mol ($Đ$ = 1.2), 11 900 g/mol ($Đ$ = 1.04), 28 300 g/mol ($Đ$ = 1.05), 74 000 g/mol ($Đ$ = 1.05), 158 000 g/mol ($Đ$ = 1.19), 522 000 g/mol ($Đ$ = 1.06) were purchased from Polymer Source Inc. PS 1 000 000 ($Đ$ = 1.05) was purchased from Agilent Technologies. Poly(2 vinylpyridine) (P2VP) 1 350 000 g/mol ($Đ$ = 1.5) was purchased from Polymer Source Inc. Polyimide (PI) 153 000 g/mol was received from Ensinger Sintimid GmbH. High molecular mass polysulfone (PSU) (proprietary) was received from Solvay. Polyethylene (PE) with M_w = 35 000 g/mol and Poly(vinylidene fluoride) (PVDF) M_w of 275 000 g/mol were purchased from Sigma-Aldrich. Toluene, *N*,*N*-Dimethylformamide, Methanol, Isopropyl Alcohol, and *p*-Xylene solvents were purchased from Sigma-Aldrich. Silicon wafers (Roughness <1 nm) were purchased from University Wafers. Eutectic Gallium Indium liquid metal alloy was purchased from Sigma-Aldrich.

Sample Preparation

The aluminum-coated electrodes were prepared by sputtering ≈100 nm aluminum on silicon wafers using ultrahigh vacuum sputtering. The polymers were dissolved in the relevant solvents (PS and PMMA in toluene, P2VP in methanol, PI and PSU in DMF), and films with different thicknesses were cast using flow coating on aluminum-coated silicon wafers. Semicrystalline PE and PVDF were dissolved in *p*-xylene and DMF respectively at high temperatures (≈100 °C) and flow coated onto heated substrates while hot. The film thicknesses were measured by using a scratch test with Bruker Dimension Icon atomic force microscope. The film annealing was performed inside a vacuum oven at 220 °C for 48 h.

Dielectric Testing

The dielectric strength of polymer films was measured using a Polyk PK-CPE1801 instrument equipped with a high-voltage trek amplifier 609D-6. The spring-loaded top electrode was softly contacted to the top of the film to make a point contact (Supporting Information Figure S1) and the bottom electrode was grounded. The electric field ramp rate was set to be 20 V/s for the films studied. Dielectric breakdown is recorded when 1 mA current passes through the film. The breakdown measurements were performed ≈15 times and the data were fit using a two-parameter Weibull analysis described by eq 2.

The frequency-dependent dielectric permittivities were calculated using a Keysight E 4980 AL LCR meter. The films were coated on aluminum-coated silicon wafers and the top electrodes were fabricated using Eutectic Gallium Indium liquid metal alloy. The electrode area was calculated by the "contact angle instrument" camera.

Optical Testing

The refractive indices were measured on films cast on silicon wafers using J. A Woolam α-SE ellipsometer and the data were fit using CompleteEASE software.

Energy Density Measurements

The gold foil (thickness ≈100 nm) was purchased from Amazon. The gold foil was dissolved in water using water-soluble tape, which resulted in small free-standing flakes (0.1 to 0.5 mm in length and breadth) of gold in water. The flakes were transferred to polymer films and sealed by vacuum. The connections to the gold foil electrodes were made using a needle hanging with a flexible metal wire to avoid puncturing the thin films. The electric displacement was measured using the PolyK PK-CPE1801 instrument at a frequency of 1 kHz.

ASSOCIATED CONTENT

Data Availability Statement

Any additional information supporting this work is available on request.

Supporting Information

The Supporting Information is available free of charge at https://pubs.acs.org/doi/10.1021/jacsau.4c00833.

Weibull probability plots; temperature-dependent dielectric strength; electrode images; breakdown spots; breakdown using wire loop electrodes; detailed comparison of nanocapacitors with literature, and additional supporting data is attached (PDF)

AUTHOR INFORMATION

Corresponding Authors

Maninderjeet Singh − *Department of Chemical and Biomolecular Engineering, University of Houston, Houston, Texas 77204, United States; Department of Chemical Engineering, Columbia University, New York, New York 10027, United States;* orcid.org/0000-0001-8891-8454; Email: ms6989@columbia.edu

Jack F. Douglas − *Material Science and Engineering Division, National Institute of Standards and Technology, Gaithersburg, Maryland 20899, United States;* orcid.org/0000-0001-7290-2300; Email: jack.douglas@nist.gov

https://doi.org/10.1021/jacsau.4c00833
JACS Au 2025, 5, 121−135

Alamgir Karim − *Department of Chemical and Biomolecular Engineering, University of Houston, Houston, Texas 77204, United States;* orcid.org/0000-0003-1302-9374; Email: akarim3@central.uh.edu

Authors

Saurabh Kr. Tiwary − *Department of Chemical and Biomolecular Engineering, University of Houston, Houston, Texas 77204, United States;* orcid.org/0000-0003-2255-7443

Roushanak Nejat − *Materials Engineering Program, University of Houston, Houston, Texas 77204, United States;* orcid.org/0000-0002-8980-507X

Complete contact information is available at: https://pubs.acs.org/10.1021/jacsau.4c00833

Author Contributions

M.S. and A.K. conceived the project. M.S. and R.N. performed the experiments. M.S. and A.K. analyzed the data. M.S. wrote the original draft. M.S., S.T., J.D., and A.K. edited the paper. CRediT: **Maninderjeet Singh** conceptualization, data curation, formal analysis, investigation, methodology, writing - original draft, writing - review & editing; **Saurabh Kumar Tiwary** validation, writing - review & editing; **Roushanak Nejat** data curation, formal analysis; **Jack F. Douglas** project administration, supervision, writing - review & editing; **Alamgir Karim** funding acquisition, project administration, writing - review & editing.

Notes

Disclaimer Certain commercial equipment, instruments, or materials are identified in this paper in order to specify the experimental procedure accurately. Such identification is not intended to imply recommendation or endorsement by the National Institute of Standards and Technology, nor is it intended to imply that the materials or equipment identified are necessarily the best available for the purpose.

The authors declare no competing financial interest.

■ ACKNOWLEDGMENTS

The authors acknowledge NSF DMR#1900692 for funding support.

■ REFERENCES

(1) Koohi-Fayegh, S.; Rosen, M. A. A Review of Energy Storage Types, Applications and Recent Developments. *J. Energy Storage* **2020**, *27*, No. 101047.

(2) Singh, M.; Apata, I.; Samant, S.; Wu, W.; Tawade, B.; Pradhan, N.; Raghavan, D.; Karim, A. Nanoscale Strategies to Enhance the Energy Storage Capacity of Polymeric Dielectric Capacitors: Review of Recent Advances. *Polym. Rev.* **2022**, *62* (2), 211−260.

(3) Singh, M.; Das, P.; Samanta, P. N.; Bera, S.; Thantirige, R.; Shook, B.; Nejat, R.; Behera, B.; Zhang, Q.; Dai, Q.; Pramanik, A.; Ray, P.; Raghavan, D.; Leszczynski, J.; Karim, A.; Pradhan, N. R. Ultrahigh Capacitive Energy Density in Stratified 2D Nanofiller-Based Polymer Dielectric Films. *ACS Nano* **2023**, *17* (20), 20262−20272.

(4) Kim, J.; Saremi, S.; Acharya, M.; Velarde, G.; Parsonnet, E.; Donahue, P.; Qualls, A.; Garcia, D.; Martin, L. W. Ultrahigh Capacitive Energy Density in Ion-Bombarded Relaxor Ferroelectric Films. *Science* **2020**, *369* (6499), 81−84.

(5) Pan, H.; Li, F.; Liu, Y.; Zhang, Q.; Wang, M.; Lan, S.; Zheng, Y.; Ma, J.; Gu, L.; Shen, Y.; Yu, P.; Zhang, S.; Chen, L. Q.; Lin, Y. H.; Nan, C. W. Ultrahigh−Energy Density Lead-Free Dielectric Films via Polymorphic Nanodomain Design. *Science* **2019**, *365* (6453), 578−582.

(6) Li, Q.; Chen, L.; Gadinski, M. R.; Zhang, S.; Zhang, G.; Li, H.; Haque, A.; Chen, L. Q.; Jackson, T.; Wang, Q. Flexible Higherature Dielectric Materials from Polymer Nanocomposites. *Nature* **2015**, *523* (7562), 576−579.

(7) Tan, D. Q. Review of Polymer-Based Nanodielectric Exploration and Film Scale-Up for Advanced Capacitors. *Adv. Funct. Mater.* **2020**, *30* (18), No. 1808567.

(8) Pan, H.; Lan, S.; Xu, S.; Zhang, Q.; Yao, H.; Liu, Y.; Meng, F.; Guo, E. J.; Gu, L.; Yi, D.; Wang, X. R.; Huang, H.; MacManus-Driscoll, J. L.; Chen, L. Q.; Jin, K. J.; Nan, C. W.; Lin, Y. H. Ultrahigh Energy Storage in Superparaelectric Relaxor Ferroelectrics. *Science* **2021**, *374* (6563), 100−104.

(9) Yang, B.; Zhang, Y.; Pan, H.; Si, W.; Zhang, Q.; Shen, Z.; Yu, Y.; Lan, S.; Meng, F.; Liu, Y.; Huang, H.; He, J.; Gu, L.; Zhang, S.; Chen, L. Q.; Zhu, J.; Nan, C. W.; Lin, Y. H. High-Entropy Enhanced Capacitive Energy Storage. *Nat. Mater.* **2022**, *21* (9), 1074−1080.

(10) Baer, E.; Zhu, L. 50th Anniversary Perspective: Dielectric Phenomena in Polymers and Multilayered Dielectric Films. *Macromolecules* **2017**, *50* (6), 2239−2256.

(11) Zhu, L.; Wang, Q. Novel Ferroelectric Polymers for High Energy Density and Low Loss Dielectrics. *Macromolecules* **2012**, *45* (7), 2937−2954.

(12) Thakur, V. K.; Gupta, R. K. Recent Progress on Ferroelectric Polymer-Based Nanocomposites for High Energy Density Capacitors: Synthesis, Dielectric Properties, and Future Aspects. *Chem. Rev.* **2016**, *116* (7), 4260−4317.

(13) Roscow, J. I.; Bowen, C. R.; Almond, D. P. Breakdown in the Case for Materials with Giant Permittivity? *ACS Energy Lett.* **2017**, *2* (10), 2264−2269.

(14) Wu, C.; Deshmukh, A. A.; Chen, L.; Ramprasad, R.; Sotzing, G. A.; Cao, Y. Rational Design of All-Organic Flexible High-Temperature Polymer Dielectrics. *Matter* **2022**, *5* (9), 2615−2623.

(15) Chen, Q.; Shen, Y.; Zhang, S.; Zhang, Q. M. Polymer-Based Dielectrics with High Energy Storage Density. *Annu. Rev. Mater. Res.* **2015**, *45*, 433−458.

(16) Alcoutlabi, M.; McKenna, G. B. Effects of Confinement on Material Behaviour at the Nanometre Size Scale. *J. Phys.: Condens. Matter* **2005**, *17* (15), No. R461, DOI: 10.1088/0953-8984/17/15/R01.

(17) Jones, R. L.; Kumar, S. K.; Ho, D. L.; Briber, R. M.; Russell, T. P. Chain Conformation in Ultrathin Polymer Films. *Nature* **1999**, *400* (6740), 146−149.

(18) Bay, R. K.; Shimomura, S.; Liu, Y.; Ilton, M.; Crosby, A. J. Confinement Effect on Strain Localizations in Glassy Polymer Films. *Macromolecules* **2018**, *51* (10), 3647−3653.

(19) Galuska, L. A.; Muckley, E. S.; Cao, Z.; Ehlenberg, D. F.; Qian, Z.; Zhang, S.; Rondeau-Gagné, S.; Phan, M. D.; Ankner, J. F.; Ivanov, I. N.; Gu, X. SMART Transfer Method to Directly Compare the Mechanical Response of Water-Supported and Free-Standing Ultrathin Polymeric Films. *Nat. Commun.* **2021**, *12* (1), No. 2347.

(20) Vignaud, G.; Chebil, M. S.; Bal, J. K.; Delorme, N.; Beuvier, T.; Grohens, Y.; Gibaud, A. Densification and Depression in Glass Transition Temperature in Polystyrene Thin Films. *Langmuir* **2014**, *30* (39), 11599−11608.

(21) Han, Y.; Huang, X.; Rohrbach, A. C. W.; Roth, C. B. Comparing Refractive Index and Density Changes with Decreasing Film Thickness in Thin Supported Films across Different Polymers. *J. Chem. Phys.* **2020**, *153* (4), No. 044902, DOI: 10.1063/5.0012423.

(22) Huang, X.; Roth, C. B. Changes in the Temperature-Dependent Specific Volume of Supported Polystyrene Films with Film Thickness. *J. Chem. Phys.* **2016**, *144* (23), No. 234903, DOI: 10.1063/1.4953855.

(23) Hamon, L.; Grohens, Y.; Holl, Y. Thickness Dependence of the Glass Transition Temperature in Thin Films of Partially Miscible Polymer Blends. *Langmuir* **2003**, *19* (24), 10399−10402.

(24) Zhao, Q.; Bennington, P.; Nealey, P. F.; Patel, S. N.; Evans, C. M. Ion Specific, Thin Film Confinement Effects on Conductivity in

Polymerized Ionic Liquids. *Macromolecules* **2021**, *54* (22), 10520−10528.
(25) Hyon, J.; Lawal, O.; Fried, O.; Thevamaran, R.; Yazdi, S.; Zhou, M.; Veysset, D.; Kooi, S. E.; Jiao, Y.; Hsiao, M. S.; Streit, J.; Vaia, R. A.; Thomas, E. L. Extreme Energy Absorption in Glassy Polymer Thin Films by Supersonic Micro-Projectile Impact. *Mater. Today* **2018**, *21* (8), 817−824.
(26) Hao, Z.; Ghanekarade, A.; Zhu, N.; Randazzo, K.; Kawaguchi, D.; Tanaka, K.; Wang, X.; Simmons, D. S.; Priestley, R. D.; Zuo, B. Mobility Gradients Yield Rubbery Surfaces on Top of Polymer Glasses. *Nature* **2021**, *596* (7872), 372−376.
(27) Zimmermann, U.; Pilwat, G.; Riemann, F. Dielectric Breakdown of Cell Membranes. *Biophys. J.* **1974**, *14* (11), 881−899.
(28) Gaylor, D. C.; Prakah-Asante, K.; Lee, R. C. Significance of Cell Size and Tissue Structure in Electrical Trauma. *J. Theor. Biol.* **1988**, *133* (2), 223−237.
(29) Fumagalli, L.; Esfandiar, A.; Fabregas, R.; Hu, S.; Ares, P.; Janardanan, A.; Yang, Q.; Radha, B.; Taniguchi, T.; Watanabe, K.; Gomila, G.; Novoselov, K. S.; Geim, A. K. Anomalously Low Dielectric Constant of Confined Water. *Science* **2018**, *360* (6395), 1339−1342.
(30) Aluru, N. R.; Motevaselian, M. H. Universal Reduction in Dielectric Response of Confined Fluids. *ACS Nano* **2020**, *14* (10), 12761−12770.
(31) Zhao, L.; Liu, C. L. Review and Mechanism of the Thickness Effect of Solid Dielectrics. *Nanomaterials* **2020**, *10* (12), No. 2473.
(32) Zhao, L.; Su, J. C.; Liu, C. L. Review of Developments on Polymers' Breakdown Characteristics and Mechanisms on a Nanosecond Time Scale. *AIP Adv.* **2020**, *10* (3), No. 035206, DOI: 10.1063/1.5110273.
(33) Neusel, C.; Schneider, G. A. Size-Dependence of the Dielectric Breakdown Strength from Nano- to Millimeter Scale. *J. Mech. Phys. Solids* **2014**, *63* (1), 201−213.
(34) Kim, H. K.; Shi, F. G. Thickness Dependent Dielectric Strength of a Low-Permittivity Dielectric Film. *IEEE Trans. Dielectr. Electr. Insul.* **2001**, *8* (2), 248−252.
(35) Wu, X.; Chen, X.; Zhang, Q. M.; Tan, D. Q. Advanced Dielectric Polymers for Energy Storage. *Energy Storage Mater.* **2022**, *44*, 29−47.
(36) Faupel, F.; Willecke, R.; Thran, A. Diffusion of Metals in Polymers. *Mater. Sci. Eng., R* **1998**, *22* (1), 1−55.
(37) Segui, Y.; Ai, B.; Bagnol, C.; Pistre, J.; Danto, Y.; Barriere, A. S. Metal Electrode Diffusion into Polymer Films. *J. Appl. Phys.* **1979**, *50* (4), 2973−2974.
(38) Sabuni, M. H.; Nelson, J. K. The Effects of Plasticizer on the Electric Strength of Polystyrene. *J. Mater. Sci.* **1979**, *14* (12), 2791−2796.
(39) Ieda, M. Dielectric Breakdown Process of Polymers. *IEEE Trans. Electr. Insul.* **1980**, *EI-15* (3), 206−224.
(40) Arun, N.; Sharma, A.; Pattader, P. S. G.; Banerjee, I.; Dixit, H. M.; Narayan, K. S. Electric-Field-Induced Patterns in Soft Viscoelastic Films: From Long Waves of Viscous Liquids to Short Waves of Elastic Solids. *Phys. Rev. Lett.* **2009**, *102* (25), No. 254502.
(41) Zhang, C.; Li, Z.; Nian, H.; Zhu, L.; Olah, A.; Baer, E. Electro-Mechanical Deformation of Amorphous and Semi-Crystalline Polymeric Films. *J. Appl. Polym. Sci.* **2020**, *137* (40), No. 49229, DOI: 10.1002/app.49229.
(42) Zhang, C.; Li, Z.; Zhu, L.; Olah, A.; Baer, E. Deformation and Failure of Polycarbonate in an Electric Field. *J. Appl. Polym. Sci.* **2020**, *137* (5), No. 48341.
(43) O'Connell, P. A.; Hutcheson, S. A.; McKenna, G. B. Creep Behavior of Ultra-Thin Polymer Films. *J. Polym. Sci., Part B: Polym. Phys.* **2008**, *46*, 1952−1965.
(44) Van Melick, H. G. H.; Govaert, L. E.; Meijer, H. E. H. On the Origin of Strain Hardening in Glassy Polymers. *Polymer* **2003**, *44* (8), 2493−2502.
(45) O'Connell, P. A.; McKenna, G. B. Rheological Measurements of the Thermoviscoelastic Response of Ultrathin Polymer Films. *Science* **2005**, *307* (5716), 1760−1763.
(46) Plazek, D. J.; Chay, I. C.; Ngai, K. L.; Roland, C. M. Viscoelastic Properties of Polymers. 4. Thermorheological Complexity of the Softening Dispersion in Polyisobutylene. *Macromolecules* **1995**, *28* (19), 6432−6436.
(47) Liu, J.; Lin, P.; Cheng, S.; Wang, W.; Mays, J. W.; Wang, S. Q. Polystyrene Glasses under Compression: Ductile and Brittle Responses. *ACS Macro Lett.* **2015**, *4* (10), 1072−1076.
(48) Yuan, G.; Li, C.; Satija, S. K.; Karim, A.; Douglas, J. F.; Han, C. C. Observation of a Characteristic Length Scale in the Healing of Glassy Polymer Interfaces. *Soft Matter* **2010**, *6* (10), 2153−2159.
(49) Xu, X.; Douglas, J. F.; Xu, W. S. Parallel Emergence of Rigidity and Collective Motion in a Family of Simulated Glass-Forming Polymer Fluids. *Macromolecules* **2023**, *56* (13), 4929−4951.
(50) Van Melick, H. G. H.; Govaert, L. E.; Meijer, H. E. H. Localisation Phenomena in Glassy Polymers: Influence of Thermal and Mechanical History. *Polymer* **2003**, *44* (12), 3579−3591.
(51) Zhu, Y.; Giuntoli, A.; Hansoge, N.; Lin, Z.; Keten, S. Scaling for the Inverse Thickness Dependence of Specific Penetration Energy in Polymer Thin Film Impact Tests. *J. Mech. Phys. Solids* **2022**, *161*, No. 104808.
(52) Constantinides, G.; Tweedie, C. A.; Holbrook, D. M.; Barragan, P.; Smith, J. F.; Van Vliet, K. J. Quantifying Deformation and Energy Dissipation of Polymeric Surfaces under Localized Impact. *Mater. Sci. Eng.: A* **2008**, *489* (1−2), 403−412.
(53) Zaccone, A.; Noirez, L. Universal G′ ∼ L-3Law for the Low-Frequency Shear Modulus of Confined Liquids. *J. Phys. Chem. Lett.* **2021**, *12* (1), 650−657.
(54) Phillips, A. E.; Baggioli, M.; Sirk, T. W.; Trachenko, K.; Zaccone, A. Universal L-3 Finite-Size Effects in the Viscoelasticity of Amorphous Systems. *Phys. Rev. Mater.* **2021**, *5* (3), No. 035602.
(55) de Gennes, P. G. Solvent Evaporation of Spin Cast Films: "Crust" Effects. *Eur. Phys. J. E* **2002**, *7* (1), 31−34.
(56) Tsige, M.; Grest, G. S. Solvent Evaporation and Interdiffusion in Polymer Films. *J. Phys.: Condens. Matter* **2005**, *17* (49), No. S4119, DOI: 10.1088/0953-8984/17/49/008.
(57) Bhattacharyya, D.; Xu, H.; Deshmukh, R. R.; Timmons, R. B.; Nguyen, K. T. Surface Chemistry and Polymer Film Thickness Effects on Endothelial Cell Adhesion and Proliferation. *J. Biomed. Mater. Res., Part A* **2010**, *94A* (2), 640−648.
(58) Zhou, J.; Berry, B.; Douglas, J. F.; Karim, A.; Snyder, C. R.; Soles, C. Nanoscale Thermal-Mechanical Probe Determination of "softening Transitions" in Thin Polymer Films. *Nanotechnology* **2008**, *19* (49), No. 495703.
(59) Wang, J.; Shi, F. G.; Nieh, T. G.; Zhao, B.; Brongo, M. R.; Qu, S.; Rosenmayer, T. Thickness Dependence of Elastic Modulus and Hardness of On-Wafer Low-k Ultrathin Polytetrafluoroethylene Films. *Scr. Mater.* **2000**, *42* (7), 687−694.
(60) Hiemenz, P. C.; Lodge, T. P. *Polymer Chemistry*; Taylor & Francis Group, 2001; Vol. *40*.
(61) Root, S. E.; Gao, R.; Abrahamsson, C. K.; Kodaimati, M. S.; Ge, S.; Whitesides, G. M. Estimating the Density of Thin Polymeric Films Using Magnetic Levitation. *ACS Nano* **2021**, *15* (10), 15676−15686.
(62) Buchdahl, R. An Interpretation of the Strength Properties of Amorphous Polymers below the Glass Transformation Temperature. *J. Polym. Sci.* **1958**, *28* (116), 239−242.
(63) Cubuk, E. D.; Ivancic, R. J. S.; Schoenholz, S. S.; Strickland, D. J.; Basu, A.; Davidson, Z. S.; Fontaine, J.; Hor, J. L.; Huang, Y. R.; Jiang, Y.; Keim, N. C.; Koshigan, K. D.; Lefever, J. A.; Liu, T.; Ma, X. G.; Magagnosc, D. J.; Morrow, E.; Ortiz, C. P.; Rieser, J. M.; Shavit, A.; Still, T.; Xu, Y.; Zhang, Y.; Nordstrom, K. N.; Arratia, P. E.; Carpick, R. W.; Durian, D. J.; Fakhraai, Z.; Jerolmack, D. J.; Lee, D.; Li, J.; Riggleman, R.; Turner, K. T.; Yodh, A. G.; Gianola, D. S.; Liu, A. J. Structure-Property Relationships from Universal Signatures of Plasticity in Disordered Solids. *Science* **2017**, *358* (6366), 1033−1037.
(64) Strickland, D. J.; Huang, Y. R.; Lee, D.; Gianola, D. S. Robust Scaling of Strength and Elastic Constants and Universal Cooperativity in Disordered Colloidal Micropillars. *Proc. Natl. Acad. Sci. U.S.A.* **2014**, *111* (51), 18167−18172.

https://doi.org/10.1021/jacsau.4c00833
JACS Au 2025, 5, 121−135

(65) Vincent, P. I. The Necking and Cold-Drawing of Rigid Plastics. *Polymer* **1960**, *1*, 7−19.
(66) Argon, A. S.; Andrews, R. D.; Godrick, J. A.; Whitney, W. Plastic Deformation Bands in Glassy Polystyrene. *J. Appl. Phys.* **1968**, *39* (3), 1899−1906.
(67) Brady, T. E.; Yeh, G. S. Y. Yielding Behavior of Glassy Amorphous Polymers. *J. Appl. Phys.* **1971**, *42* (12), 4622−4630.
(68) Grenet, J.; G'Sell, C. Observation and Modelling of Shear-Band Propagation in Glassy Polycarbonate. *Polymer* **1990**, *31* (11), 2057−2065.
(69) Wu, P. D.; van der Giessen, E. On Neck Propagation in Amorphous Glassy Polymers under Plane Strain Tension. *Int. J. Plast.* **1995**, *11* (3), 211−235.
(70) Donald, A. M.; Kramer, E. J. The Competition between Shear Deformation and Crazing in Glassy Polymers. *J. Mater. Sci.* **1982**, *17* (7), 1871−1879.
(71) Kramer, E. J. Open Questions in the Physics of Deformation of Polymer Glasses. *J. Polym. Sci., Part B: Polym. Phys.* **2005**, *43* (23), 3369−3371.
(72) Wang, S. Q. The Tip of Iceberg in Nonlinear Polymer Rheology: Entangled Liquids Are "Solids. *J. Polym. Sci., Part B: Polym. Phys.* **2008**, *46* (24), 2660−2665.
(73) Roth, C. B. *Polymer Glasses*; CRC Press, Taylor & Francis Group, 2016.
(74) Govaert, L. E.; Tervoort, T. A. Strain Hardening of Polycarbonate in the Glassy State: Influence of Temperature and Molecular Weight. *J. Polym. Sci., Part B: Polym. Phys.* **2004**, *42* (11), 2041−2049.
(75) Deblieck, R. A. C.; Van Beek, D. J. M.; Remerie, K.; Ward, I. M. Failure Mechanisms in Polyolefines: The Role of Crazing, Shear Yielding and the Entanglement Network. *Polymer* **2011**, *52* (14), 2979−2990.
(76) Singh, M.; Dong, M.; Wu, W.; Nejat, R.; Tran, D. K.; Pradhan, N.; Raghavan, D.; Douglas, J. F.; Wooley, K. L.; Karim, A. Enhanced Dielectric Strength and Capacitive Energy Density of Cyclic Polystyrene Films. *ACS Polym. Au* **2022**, *2* (5), 324−332.
(77) Tawade, B. V.; Singh, M.; Apata, I. E.; Veerasamy, J.; Pradhan, N.; Karim, A.; Douglas, J. F.; Raghavan, D. Polymer-Grafted Nanoparticles with Variable Grafting Densities for High Energy Density Polymeric Nanocomposite Dielectric Capacitors. *JACS Au* **2023**, *3* (5), 1365−1375.
(78) Singh, M.; Agrawal, A.; Wu, W.; Masud, A.; Armijo, E.; Gonzalez, D.; Zhou, S.; Terlier, T.; Zhu, C.; Strzalka, J.; Matyjaszewski, K.; Bockstaller, M.; Douglas, J. F.; Karim, A. Soft-Shear-Aligned Vertically Oriented Lamellar Block Copolymers for Template-Free Sub-10 Nm Patterning and Hybrid Nanostructures. *ACS Appl. Mater. Interfaces* **2022**, *14* (10), 12824−12835.

https://doi.org/10.1021/jacsau.4c00833
JACS Au 2025, 5, 121−135